



## Application of electrospinning to fabricate phycocyanin- and *Spirulina* extract-loaded gliadin fibers for active food packaging

Mohammad-Taghi Golmakani<sup>\*</sup>, Mohammad Mahdi Hajjari, Farzaneh Kiani, Niloufar Sharif, Seyed Mohammad Hashem Hosseini

Department of Food Science and Technology, School of Agriculture, Shiraz University, Shiraz, Iran

### ARTICLE INFO

#### Keywords:

Active food packaging  
Electrospinning  
Gliadin  
Phycocyanin  
*Spirulina* extract

### ABSTRACT

This study explored the active food packaging application of phycocyanin- and *Spirulina* extract-loaded gliadin electrospun fibers (GPhy and GSPE<sub>5%</sub>). SEM findings confirmed that the morphology of fibers was tubular, showing the GPhy and GSPE<sub>5%</sub> as the optimum fibers. The loading efficiencies of GPhy and GSPE<sub>5%</sub> were also around 90%, which proved the well-incorporated compounds within the fibers. Simulation results of  $\alpha$ -gliadin dissolved in acetic acid illustrated the denaturation of the protein. FTIR and TGA confirmed that after electrospinning the chemical/structural changes and enhanced thermostabilities occurred, respectively. Antibacterial and antioxidant tests detected higher bactericidal and antioxidative effects of GSPE<sub>5%</sub> than GPhy. In the application part, it was found that GPhy and GSPE<sub>5%</sub> were able to decrease PV and TBA values as the indications of walnut kernels' protection from lipid oxidation. This work shows a facile and an efficient way to fabricate active food packaging materials using electrospinning and natural compounds.

### 1. Introduction

Active food packaging is a unique approach to extend the shelf life of food products along with the simultaneous guarantee of their quality during storage and distribution (Ge, Huang, Zhou, & Wang, 2022). Although synthesized plastic materials are usually preferred for food packaging and transportation, the utilization of bioactive-loaded active packaging films from natural sources have drawn many attentions in recent years because of the increments in public awareness on health and environmental impacts (Sharif, Golmakani, Hajjari, Aghaee, & Ghasemi, 2021). The risk level of chemical (organic and inorganic) and microbial food contaminations varies with the amount of food consumed and the quantity of contaminants. Generally, the methods to prevent contaminations are from pre-harvest to post-harvest steps. Nonetheless, packaging systems such as smart and active food packagings are known as prevailing protective layers against external hazards (Alum, Urom, & Ben, 2016; Onyeaka et al., 2024). The most common active packaging materials provide bactericidal and antioxidative impacts against microbial and chemical spoilage (Kuai et al., 2021). In addition to this, it has been proven that the incorporation of bioactive compounds preserves or improves their thermal and structural stabilities (Neo et al., 2013). Some of the notable methods for the fabrication of

active food packaging materials can be electrohydrodynamic, solvent casting, extrusion, thermoforming, and compression molding. Compared to the mentioned techniques, electrohydrodynamic methods consisting of electrospinning and electrospraying are versatile and facile manners to form fibers and particles from biopolymer solutions (Ghorani & Tucker, 2015). When it comes to electrospun biopolymers, many studies have demonstrated fibers made from carbohydrates (e.g. cellulose, cellulose derivatives, and chitosan) and proteins (e.g. zein, gliadin, and gelatin) (Kumar & Sinha-Ray, 2018). Gliadin, as an alcohol-soluble glycoprotein from wheat kernel, can be divided to four groups of  $\alpha$ -,  $\beta$ -,  $\gamma$ -, and  $\omega$ -gliadins. Interestingly, these proteins are different in shape as  $\gamma$ - and  $\omega$ -gliadins are rod-like substructures (Hajjari & Sharif, 2021). It is worth noting that the promising results on the electrospun gliadin for the encapsulation of bioactive molecules have been also reported. Akman, Bozkurt, Balubaid, Yilmaz, and Polymers (2019); Chen et al. (2023); Hajjari, Golmakani, and Sharif (2021) investigated electrospun curcumin-loaded, cuminoldehyde-loaded, and chlorogenic acid gliadin fibers to provide antimicrobial and/or antioxidative effects, respectively. Their studies were also capable of proving that the electrospun gliadin has potent potentiality to encapsulate bioactive molecules.

*Spirulina* is a valuable source of proteins and antioxidative compounds. The extract may contain high protein content of 60–70% by dry

<sup>\*</sup> Corresponding author at: Department of Food Science and Technology, School of Agriculture, Shiraz University, Shiraz 7144165186, Iran.

E-mail addresses: [golmakani@shirazu.ac.ir](mailto:golmakani@shirazu.ac.ir) (M.-T. Golmakani), [hosseini@shirazu.ac.ir](mailto:hosseini@shirazu.ac.ir) (S.M.H. Hosseini).

weight and 30–40% of vitamins, essential fatty acids, carotenoids, antioxidants, and phycocyanin. The free radical scavenging activity of *Spirulina* is believed to be the sum of effects given by phycocyanin,  $\beta$ -carotene, and other vitamins and minerals (Kumar et al., 2022). Usharani, Srinivasan, Sivasakthi, and Saranraj (2015) stated that the antioxidant and antibacterial effects of *Spirulina* extract might be connected to the presence of high amounts of phenolic compounds. They also mentioned that *Spirulina* extract possesses higher content of phenolic compounds than another commercial alga named *Chlorella*, which can further results in better antioxidant and antibacterial activities. Phycocyanin, as a pigment-protein complex, comprises 20% of total proteins in *Spirulina*. However, the content of phycocyanin strongly depends on extraction solvent and method (Fernandes et al., 2023). It is worth noting that phycocyanin is able to indicate decent bacterial and antioxidative performances by itself (Mohamed, Osman, Abo Eita, & Sitohy, 2018). These active compounds may enable researchers to reduce the concerns about food products with high levels of polyunsaturated fatty acids for their susceptibility to lipid oxidation. Walnut kernel is naturally an enormous source of polyunsaturated fatty acids. This feature causes the instability of walnut kernels by lipid oxidation and rancidity, which usually results in impossible long-time storage and complicated food applications (Poggetti, Ferfuaia, Chiabà, Testolin, & Baldini, 2018). Nevertheless, there have been reports on the extension of walnut kernels' shelf-life by means of antioxidant coatings such as gallic acid-loaded hydroxypropyl methylcellulose electrospun fibers by Aydogdu et al. (2019) and gallic acid-loaded lentil flour-based electrospun fibers by Aydogdu, Sumnu, and Sahin (2019).

The main objective of the present study was to investigate the packaging application of electrospun gliadin fibers containing *Spirulina* extract and phycocyanin on walnut kernels during the storage period. Nonetheless, gliadin simulation, its physicochemical properties, and antibacterial and antioxidant effects of loaded-fibers were also studied. It is essential to mention that, when necessary, comparisons between fibers containing *Spirulina* extract and phycocyanin were made.

## 2. Materials and methods

### 2.1. Materials

Pure ethanol, methanol, hexane, and chloroform were obtained from Pars Alcohol Company (Eghlid, Iran). *Spirulina* was purchased from Swisse (Melbourne, Australia). Phycocyanin, glacial acetic acid, trichloroacetic acid, thiobarbituric acid, aluminum chloride (10%), sodium carbonate, potassium acetate, butylated hydroxytoluene (BHT), gallic acid, quercetin, Folin-Ciocalteu reagent, sodium 1,2-naphthoquinone-4-sulfonate, 2,2-diphenyl-1-picrylhydrazyl (DPPH), and tryptic soy agar (TSA) were gained from Sigma-Aldrich (St. Louis, MO).

### 2.2. Gliadin and *Spirulina*

#### 2.2.1. Gliadin extraction

Gliadin was extracted from wheat gluten using the method of Sharif, Golmakani, and Hajjari (2022) with negligible modifications. Accordingly, 20 mg of wheat gluten was dissolved in 250 mL of ethanol 70% for 3 h. The mixture was centrifuged using a centrifugation speed of 7500 rpm at 15–20 °C for 10 min. The purity of the obtained gliadin was measured to be ~90%, according to the Kjeldahl technique.

#### 2.2.2. *Spirulina* extraction

Concentrated *Spirulina* extract was prepared by mixing *Spirulina* with ethanol 70% with a concentration of 0.1 g/mL. Then, it was stirred and kept at 55 °C to obtain a uniform solution. Then, it was incubated at 40–45 °C for 24 h. The resultant solution was filtered via Whatman filter papers after centrifuging at a speed of 7500 rpm for 10 min at 10 °C. As the final preparation step of concentrated *Spirulina* extract (SPE), a rotary evaporator was used at 35 °C for 30 min (Moreira et al., 2019). The

moisture content of SPE was also analyzed (~14%).

#### 2.2.3. Phenols and flavonoids content

The total amount of phenols present in SPE was measured via Folin-Ciocalteu reagent method. In brief, 0.75 mL of 10% Folin-Ciocalteu reagent was dissolved in 0.10 mL of SPE with different dilutions. Then, 0.75 mL of 2% sodium carbonate was mixed. After 45 min, the absorbance of the solution was read at 765 nm. In addition, the control sample was of 0.1 mL of ethanol 70% and calibration curve was plotted via gallic acid standards in a range of 0.01 to 0.1 mg/mL (Lu et al., 2011).

The total amount of flavonoids in SPE was studied by the aluminum chloride colorimetric method. Briefly, SPE solutions of various dilutions were mixed with 1.5 mL of ethanol 70%, 0.1 mL of 10% aluminum chloride, 0.1 mL of 1 mol/L potassium acetate, and 2.8 mL of distilled water. After 30 min, the absorbance value of each mixture was read at 415 nm. The calibration curve was of quercetin standards in a range of 0.01 to 0.1 mg/mL (Choudhary, Tanwer, Singh, & Vijayvergia, 2013). According to the methods, total phenols and total flavonoids in dried and fresh SPE with a concentration of 0.1 mg/mL were ~ 203, ~41 mg<sub>phenols</sub>/g<sub>SPE</sub>, ~135, and ~ 27 mg<sub>flavonoids</sub>/g<sub>SPE</sub>, respectively.

#### 2.2.4. Phycocyanin content

Phycocyanin content was measured via the separation of liquid and solid phases when 20 mL of SPE was centrifuged at 4000 rpm for 10 min, followed by reading the absorbance values at 615 and 652 nm by the following equation (Hajjari, Golmakani, & Sharif, 2023):

$$\text{Phycocyanin content (mg/mL)} = ((A_1 - (0.474 \times A_2)) / 5.34) \quad (1)$$

where  $A_1$  and  $A_2$  were the absorbance values at 615 and 652 nm, respectively.

Accordingly, the fresh and dried SPE indicated ~17% and 20% phycocyanin content, respectively.

## 2.3. Electrospinning

### 2.3.1. Electrospinning solutions

Uniform gliadin solutions were made at an optimum concentration of 25% using glacial acetic acid. Then, SPE at various concentrations of 2%, 5%, 8%, and 10% and phycocyanin at a concentration of 5% were added. Rheological properties of solutions were measured by a viscometer (MCR-302, Anton Paar, Austria), conductivity meter (C933, De Bruyne Instruments, Belgium), and tensiometer (Contact angle-101, Nano Metric, Iran).

### 2.3.2. Electrospinning method

Electrospun fibers were obtained from an electrospinner machine (Spinner-3×-Advance, ANSTCO, Iran). During the process, a voltage of 15 kV was set from a distance of 10 cm from an aluminum-coated collector. Moreover, a flow rate of 0.5 mL/h was set for the process. The fibers gained from gliadin solutions with and without phycocyanin and SPE were named GL (pure gliadin solution), GPhy (gliadin solution with 5% phycocyanin), and GSPE<sub>x</sub> (gliadin solutions with 2%, 5%, 8%, and 10% SPE; x is the percentage of concentrations).

## 2.4. Electrospun fibers

### 2.4.1. Morphology of fibers

SEM (TESCAN, Brno, Czech Republic) visualized the samples at a scale of 10  $\mu$ m. Digimizer as an image analyzer (Version 5.3.5, Ostend, Belgium) was used to measure the diameter of fibers. Moreover, loading efficiencies were calculated (Eq. (2)) based on the phycocyanin content obtained from Eq. (1) (mg) and the hypothetical amounts of added compounds (mg). In this method, samples were dissolved in PBS with a concentration of 2 mg/mL.

$$\text{Loading efficiency (\%)} = ((A_1 - (0.474 \times A_2)) / 5.34) / (H_A) \times 100 \quad (2)$$

where  $A_1$  and  $A_2$  were the absorbance values at 615 and 652 nm, respectively, and  $H_A$  was the hypothetical amounts of added compounds (mg).

#### 2.4.2. Gliadin modeling and simulation

Three-dimensional  $\alpha$ -gliadin substructure was generated using on-line servers for ab initio modeling (Xu & Zhang, 2012) by the means of FASTA sequence. The protein was checked via SWISS-MODEL server to confirm the structural accuracy (Benkert, Biasini, & Schwede, 2011). In order to simulate the acidic effects of acetic acid molecules on gliadin, the protein was protonated using the protonation state computed by H++ server (Anandakrishnan, Aguilar, & Onufriev, 2012). Then, gliadin was placed in the center of a cubic box with the periodic boundary conditions, which had the equal distances of 1 nm among edges and the central protein. The box was filled with acetic acid molecules. Ionic neutralization and energy minimization were carried out by chloride ion and the steepest descent method, respectively. The NVT and NPT ensembles were carried out at a constant temperature of 300 K and constant pressure of 1 bar for 500 ps, respectively. The pressure was constant at 1 bar via runs of Berendsen and Parrinello Rahman barostat. Eventually, the 50 ns MD simulation with a force field of GROMOS 54A7 was carried out using GROMACS (University of Groningen, Version 2019.6, Groningen, Netherlands). All protein structures were visualized by VMD (University of Illinois Urbana-Champaign, Version 1.9.3, Champaign, IL). MD results were analyzed based on the comparison of initial and final models and the residues fluctuation that studied by RMSD and RMSF values, respectively. Moreover, the protein unfolding and secondary structure were evaluated by radius of gyration ( $R_g$ ) and secondary structure (DSSP algorithm). In the simulation section, the simulated  $\alpha$ -gliadin was named GL.

#### 2.4.3. FTIR and TGA

FTIR (Tensor II, Bruker, Germany) in a range of 4000 to 400  $\text{cm}^{-1}$  was performed to assay the functional groups as well as the chemical and structural changes of the samples. TGA (DSC/TGA1, Mettler Toledo, Switzerland) was to study the thermostability of the samples. Hence, thermograms from 30 to 600 °C were plotted to evaluate the thermostability of the samples.

#### 2.5. Antioxidant activity

Antioxidative effect of fibers were studied using DPPH method (Hajjari et al., 2023). In this regard, fibers were dissolved in methanol 70% solution with a concentration of 6 mg/mL. Moreover, DPPH solution had a 0.1 mmol/L concentration. The absorbance values of samples were read at 517 nm and the values were used as the inputs of the following equation:

$$\text{Antioxidative effect (\%)} = ((A_C - A_F) / (A_C)) \times 100 \quad (3)$$

where  $A_C$  and  $A_F$  were the absorbance values of the control and fibers, respectively.

#### 2.6. Antimicrobial activity

Antibacterial effects were tested on *Staphylococcus aureus* and *Escherichia coli* bacteria. The method was disk diffusion reported by Sharif et al. (2021), where the inhibition zones of bactericidal effects were measured. Firstly, a PBS solution with  $10^6$  CFU/mL of bacteria was made and set to McFarland's standard as it required an absorbance in a range of 0.08–0.1 at 600 nm. Then, 100  $\mu\text{L}$  of bacterial suspension was spread on TSA medium plates. For tested plates, UV-sterilized fibers with a dimension of  $2 \times 2 \text{ cm}^2$  were placed in the center of TSA plates as disks. The incubation was used to keep the plates at 37 °C for 24 h. Finally, the

diameter of inhibition zones was measured.

#### 2.7. Packaging application

##### 2.7.1. Oxidative potentiality

To confirm the oxidative potentiality of samples, it was required to measure the oil efficiency of walnut kernels. Hence, a certain amount (10 g) of walnuts were wrapped with filtration papers. Then, Hexane was mixed with the coated walnuts. The samples were kept in a Soxhlet system for 3 h and subsequently they were kept in an oven with a temperature of 40 °C for 24 h to evaporate all hexane molecules. The oil efficiency was measured via the weight difference before and after the applied method.

##### 2.7.2. Accelerated packaging test

During a 15-week accelerated storage test, 30 mg of electrospun fibers coated 20 g of walnut samples. Then, they were kept at a constant temperature of 60 °C to indicate the potential antioxidative packaging application (Sabbaghi & Mehravar, 2015).

##### 2.7.3. Peroxide value

Peroxide value (PV) of samples was to indicate the primary oxidation products during storage period. Firstly, 0.001–0.03 g of hexane-extracted walnut oil was mixed with 9.8 mL of chloroform:methanol solution in a ratio of 7:3. Secondly, the mixture was blended with 50  $\mu\text{L}$  of ammonium thiocyanate and 50  $\mu\text{L}$  of iron chloride. Eventually, the final solution was mixed with 100  $\mu\text{L}$  of HCl (10 mol/L) to form sediments. The absorbance was measured at 500 nm and the value was the input of the following equation (Sabaghi, Maghsoudlou, Khomeiri, & Ziaifar, 2015):

$$\text{Peroxide value} = ((A_S - A_C) \times S) / (\text{amu}_{\text{Fe}} \times 2 \times m_S) \quad (4)$$

where  $A_S$ ,  $A_C$ ,  $S$ ,  $\text{amu}_{\text{Fe}}$ , and  $m_S$  are absorbance values of the sample and control, slope obtained from the calibration curve (41.52), atomic mass of iron (55.84), and the mass of the sample (g), respectively.

##### 2.7.4. Thiobarbituric acid value

The thiobarbituric acid (TBA) test was applied to measure the secondary oxidation products of walnut kernel oil during the storage period. In other words, the TBA value indicates the measurement of lipid oxidation based on malondialdehyde content. The TBA method included the step of dissolving 15 g of trichloroacetic acid in 0.336 g of thiobarbituric acid, 1.76 mL of 12 mol/L HCl, and 82.8 g of distilled water. Then, the solution was mixed with 3 mL of 2% butylated hydroxytoluene:ethanol with a ratio of 1:1. The new solution was kept in boiling water bath for 15 min and a phase separation was subsequently performed by centrifugation at the speed of 3500 rpm for 10 min. Eventually, the absorbance value of liquid phase was read at 532 nm (Sharma et al., 2018).

#### 2.8. Statistical analysis

All results were reported with mean value  $\pm$  standard deviation of at least triplicate determinations ( $n \geq 3$ ). SPSS 26 statistical software (SPSS Inc., Chicago, IL) was used to evaluate statistical analyses via one-way ANOVA with Tukey's post-hoc test. Duncan's multiple range test with a 95% level of confidence ( $P < 0.05$ ) was used to measure the significant differences.

### 3. Results and discussion

#### 3.1. Morphology

The fibers' morphology is immensely dependent on the conditions of the solution and electrospinning method. Although the method's

parameters were the same for all samples, any changes in the morphology of the fibers were certainly the results of differences among the solutions properties. Findings are indicated in Fig. 1 and Table 1. As a first impression, all images confirmed that fibers had the tubular morphology. Hajjari et al. (2023) stated that this morphology is common when an acidic solvent is used for preparation of the solution. They attributed this tubular morphology to the denaturation of protein, which resulted from the formation of hydrogen bonding with solvent molecules. Moreover, as illustrated in Fig. 1, only GL, GPhy, GSPE<sub>2%</sub>, and GSPE<sub>5%</sub> were smooth and beadless samples. Generally, decreases in surface tension, increments in conductivity, and higher values of viscosity can provide thin, smooth, and unbeaded fibrous structures, respectively. However, improper values of viscosity, as the predominant factor of solution properties, might cause bigger beads on thicker fibers (Ghorani & Tucker, 2015). This also could be why only GL, GPhy, GSPE<sub>2%</sub>, and GSPE<sub>5%</sub> had showed unbeaded structures. This point is crucial to mention that GPhy had the same amounts of concentration with GSPE<sub>5%</sub>, however, it showed higher viscosity values. According to Hajjari, Golmakani, Sharif, and Niakousari (2021), the plasticizers can inhibit entanglements between biopolymers, resulting in lower values of viscosity. SPE-loaded samples clearly possessed more plasticizers and less proteins content. Despite the variations in solution properties, fibers had the same morphology and diameter. Accordingly, GL (561 ± 173 nm), GPhy (464 ± 165 nm), and GSPE<sub>5%</sub> (423 ± 127 nm) have been chosen for further evaluations. Additionally, the loading efficiencies of GPhy and GSPE<sub>5%</sub> were 90.3 ± 3.27% and 91.1 ± 4.12%, respectively. These values were the indications of well incorporation into the gliadin

**Table 1**

Properties of the solutions and electrospun fibers.

Solution of	Surface tension (mN.m <sup>-1</sup> )	Conductivity (μs.cm <sup>-1</sup> )	Viscosity (mPa.s)	Diameter (nm)
GL*	31.56 ± 0.79 <sup>a</sup>	145.25 ± 1.76 <sup>a</sup>	162.33 ± 10.65 <sup>a</sup>	561 ± 173 <sup>a</sup>
GPhy*	35.53 ± 0.52 <sup>b</sup>	147.60 ± 1.55 <sup>b</sup>	236.70 ± 3.48 <sup>b</sup>	464 ± 165 <sup>a</sup>
GSPE <sub>2%</sub>	31.52 ± 0.34 <sup>a</sup>	143.10 ± 1.97 <sup>a</sup>	165.07 ± 6.12 <sup>a</sup>	417 ± 146 <sup>a</sup>
GSPE <sub>5%</sub> *	31.22 ± 0.41 <sup>a</sup>	144.35 ± 3.74 <sup>ab</sup>	202.79 ± 4.65 <sup>c</sup>	423 ± 127 <sup>a</sup>
GSPE <sub>8%</sub>	31.18 ± 0.57 <sup>a</sup>	146.40 ± 0.84 <sup>ab</sup>	205.90 ± 3.05 <sup>c</sup>	Beaded
GSPE <sub>10%</sub>	28.80 ± 0.37 <sup>c</sup>	147.65 ± 1.06 <sup>ab</sup>	212.09 ± 2.13 <sup>d</sup>	Beaded

\* Solutions which demonstrated optimum electrospun fibers. Means with different letters show the significant difference ( $P < 0.05$ ). GL, GPhy, and GSPE<sub>2%</sub>, 5%, 8% and 10% were pure gliadin fiber, phycocyanin-loaded gliadin fiber, and gliadin fibers containing 2%, 5%, 8%, and 10% *Spirulina* extract, respectively.

fibers.

### 3.2. Physicochemical properties

Fig. 2a indicates the gliadin three-dimensional structure in acetic acid. As shown in Fig. 2a, the gliadin was obviously unfolded and elongated in comparison with its initial form. Generally, increases in

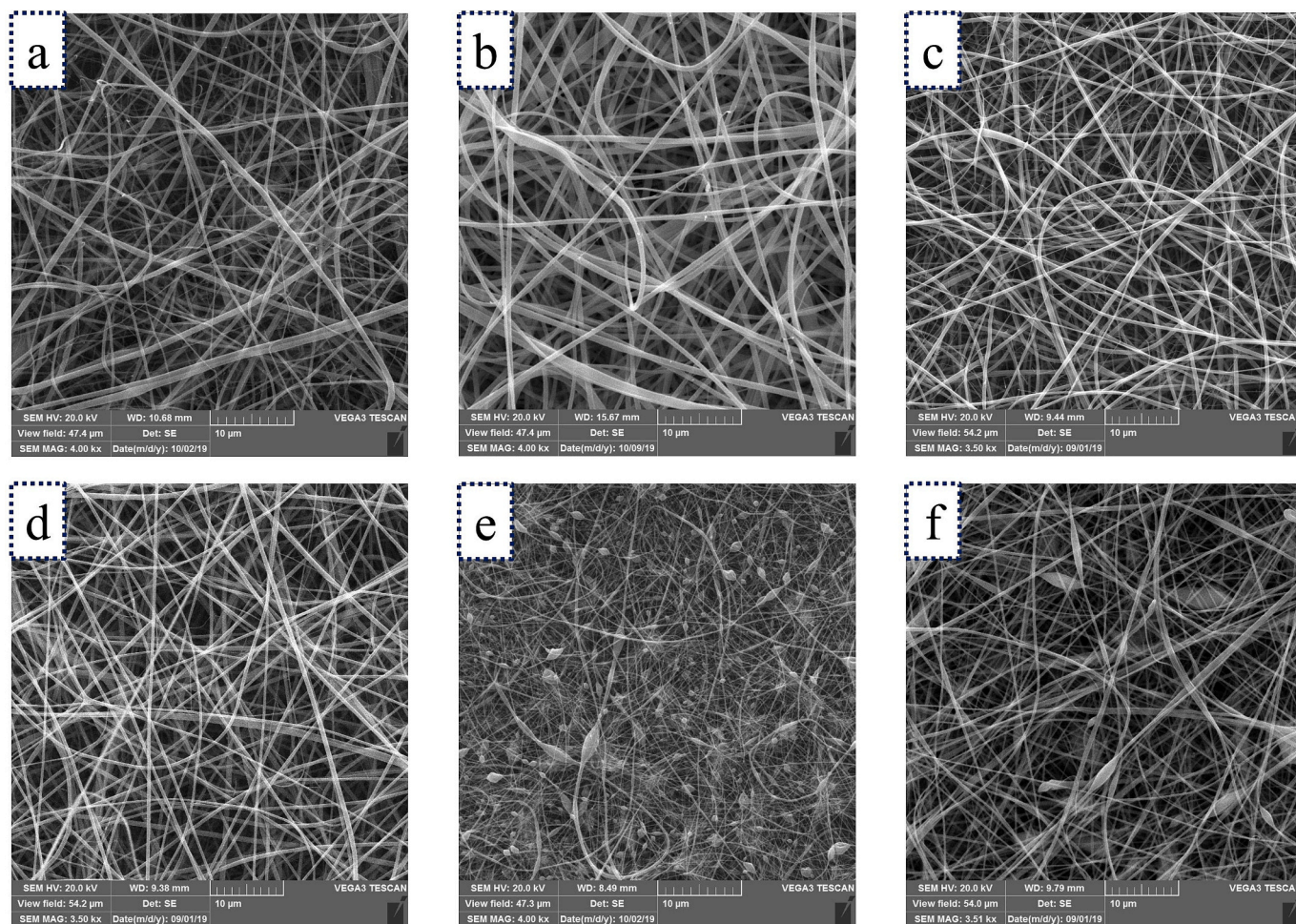


**Fig. 1.** SEM images of (a) GL, (b) GPhy, (c) GSPE<sub>2%</sub>, (d) GSPE<sub>5%</sub>, (e) GSPE<sub>8%</sub>, and (f) GSPE<sub>10%</sub>. GL, Gphy, and GSPE<sub>2%</sub>, 5%, 8%, and 10% were pure gliadin fiber, phycocyanin-loaded gliadin fiber, and gliadin fibers containing 2%, 5%, 8%, and 10% *Spirulina* extract, respectively.

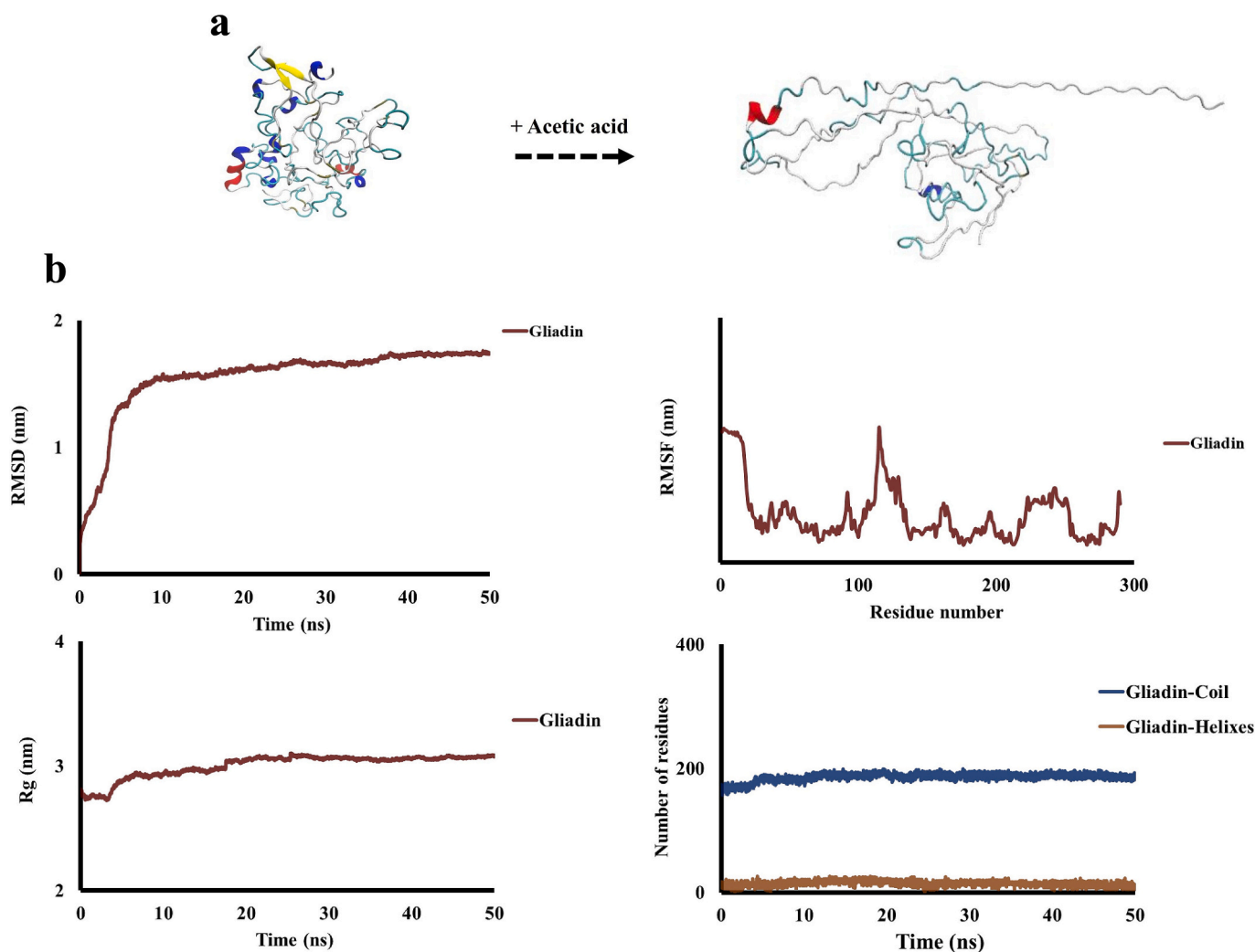


Fig. 2. (a) VMD image of gliadin before and after the effects of acetic acid. (b) RMSD, RMSF,  $R_g$ , and secondary structure of gliadin during denaturation.

RMSD and high fluctuations in RMSF demonstrate proteins' instability, which can be owing to the dissolution or stresses (Srinivas, Ochiye, & Mohan, 2014). In addition, increases in  $R_g$  is related to the proteins' unfolding (Hajjari & Sharif, 2022). In Fig. 2b, both RMSD and RMSF were able to show how gliadin was destabilized in acetic acid. Moreover,  $R_g$  proved that gliadin was also elongated/unfolded during dissolution.

This can be connected to the denaturation term, which is common in proteins' structural changes. Secondary structure curves of gliadin were also in accordance with other findings. It indicated that the helical and coiled domains of gliadin increased and decreased, respectively. Principally, unfolding caused by dissolving, electric field and stresses provides more coiled domains.

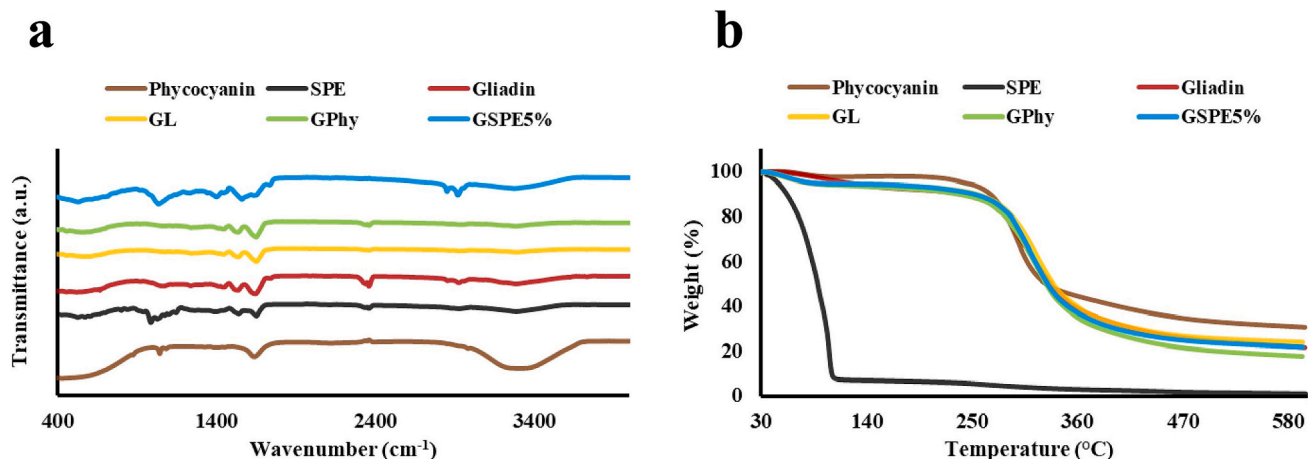


Fig. 3. (a) FTIR spectra and (b) TGA thermograms of proteins and fibers.

Fig. 3a and Fig. 3b possess the FTIR spectra and TGA thermograms of the samples. Proteins usually show characteristic peaks at  $\sim 3200$ , 1650, 1530, and  $1450\text{ cm}^{-1}$  for amides A, I, II, and III, respectively (Akman, Bozkurt, Balubaid, & Yilmaz, 2019). Phycocyanin have some specific peaks beside its protein fingerprints (amides) in a range of  $800\text{--}1000\text{ cm}^{-1}$  that could be of C—O stretching and linker S—CH bands (Chentir et al., 2018). Spirulina extract, as a mixture of various compounds, particularly displays halo and sharp peaks at  $3200\text{--}2800$ ,  $1600\text{--}1500$ , and  $1300\text{--}1000\text{ cm}^{-1}$  as indications of lipids, proteins, and carbohydrates, respectively (Kavitha, Stephen, Brishti, & Karthikeyan, 2021). According to Fig. 3a, findings of FTIR properly followed the mentioned patterns, however, they had some negligible differences. Negligible shifts appeared at higher wavenumbers for amide II bands after electrospinning of proteins (from  $\sim 1650\text{ cm}^{-1}$  of pure structures to  $\sim 1660\text{ cm}^{-1}$  of electrospun samples). These changes were expected to state the changes in molecular conformation (Hajjari, Golmakani, & Sharif, 2021). Moreover, majority of distinctive peaks of SPE and phycocyanin were combined with gliadin peaks in GPhy and GSPE<sub>5%</sub> spectra, which might be related to the proper incorporation. Fig. 3b shows TGA thermograms of samples. The thermograms of proteins usually have two degradations regions during heating up in the ranges of  $80\text{--}160$  and  $230\text{--}420\text{ }^\circ\text{C}$ , respectively. It is considered that the first and second degradations of proteins are the reasons of the evaporation of volatile compounds/unbound water molecules and protein decomposition, respectively (Moreno, Orqueda, Gómez-Mascaraque, Isla, & López-Rubio, 2019). All protein-based samples of this study had two degradations. However, GSPE<sub>5%</sub> and GL claimed the a little more thermostability than GPhy because of the delayed second degradation and more residual matter. However, among all samples, SPE had the least thermal stability limited to the nearly first degradation. The second degradation was shown with a gradual decrease until  $600\text{ }^\circ\text{C}$ , degrading proteins and carbohydrates at  $200\text{--}350\text{ }^\circ\text{C}$  and lipids at  $350\text{--}600\text{ }^\circ\text{C}$  (Larrosa et al., 2018). In this regard, GSPE<sub>5%</sub> was appropriately able to overcome the thermo-susceptibility of SPE.

### 3.3. Antimicrobial and antioxidant effects

Table 2 indicates the antioxidative and bactericidal activities of the samples. The inhibition zones of  $4.5 \pm 0.5\text{ mm}$  ( $\sim 7.5\%$ , diameter of inhibition zone per diameter of petri dish) and  $6.0 \pm 0.3\text{ mm}$  ( $\sim 10\%$ , diameter of inhibition zone per diameter of petri dish) against *S. aureus* were shown for GPhy and GSPE<sub>5%</sub>, respectively. However, *E. coli* showed less susceptibility to the loaded-fibers and therefore the inhibition zones of GPhy and GSPE<sub>5%</sub> progressed to only  $1.3 \pm 0.5\text{ mm}$  ( $\sim 2.1\%$  diameter of inhibition zone per diameter of petri dish) and  $2.4 \pm 0.2\text{ mm}$  ( $\sim 4\%$  diameter of inhibition zone per diameter of petri dish), respectively. Hence, these findings could point out the hydrophilic LPS as the exterior layer of Gram-negative bacteria. This layer hinders the diffusion and penetration of macromolecules and hydrophobic compounds into the bacteria cells (Walker & Black, 2021). Moreover, based on the comparisons between GPhy and GSPE<sub>5%</sub>, it was observed that SPE was more microbiologically inhibitor against Gram-positive and -negative bacteria than phycocyanin sample. It could be owing to some compounds present in SPE such as phenols. Phenols generally can cause the leakage of intracellular constituents in addition to the inhibitory

**Table 2**  
Antioxidative and bactericidal effects of loaded fibers.

Sample	Antioxidative effect (%)	Bactericidal effect (mm)	
		<i>Staphylococcus aureus</i>	<i>Escherichia coli</i>
GPhy	$21.72 \pm 2.44^a$	$4.5 \pm 0.5^a$	$1.3 \pm 0.5^a$
GSPE <sub>5%</sub> *	$30.51 \pm 3.32^b$	$6.0 \pm 0.3^b$	$2.4 \pm 0.2^b$

Means with different letters show the significant difference ( $P < 0.05$ ). GPhy and GSPE<sub>5%</sub> were phycocyanin-loaded gliadin fiber and gliadin fibers containing 5% Spirulina extract, respectively.

effects against the bacterial growth (Park et al., 2001). Similarly, phycocyanin shows its mode of action by the creation of channels on the cells' membrane to eliminate bacteria by cellular leakage phenomenon (Mohamed et al., 2018). In Table 2, GPhy and GSPE<sub>5%</sub> had the free radical scavenging activities of  $21.72 \pm 2.44\%$  and  $30.51 \pm 3.32\%$ , respectively. According to Asghari, Fazilati, Latifi, Salavati, and Choo-pani (2016), SPE is capable of demonstrating the antioxidant activity using phenols, flavonoids, phycocyanin,  $\beta$ -carotene, and chlorophyll. Antioxidant effects of phycocyanin is mainly connected with the residues of chromatophore phycocyanobilin and phycocyanopeptide that decrease oxidation probability (Mohamed et al., 2018). Although GPhy possessed higher amounts of phycocyanin than GSPE<sub>5%</sub>, SPE-loaded sample was more antioxidative. In this regard, the combination of phycocyanin with the synergistic effects of phenols and flavonoids enhanced the GSPE<sub>5%</sub> activity (Hajimehdipoor, Shahrestani, & Shekarchi, 2014).

### 3.4. Oxidative stability

The 15-week storage test is shown in Fig. 4a. During the test, curves showed gradual increases over 15 weeks of storage from the first ( $2.5 \pm 0.31\text{ meq/kg}$ ) to 9th (from the highest of  $10.64 \pm 0.77$  to the lowest of  $7.50 \pm 0.57\text{ meq/kg}$ ) week intervals. In contrast, a downward approach was observed from 9th to 15th week intervals. Hence, the process met the break point of PV in 9th week. Based on comparison, the oxidation level of coated samples (GL, GPhy, and GSPE<sub>5%</sub>) before the break point was lower than the control sample. This can be owing to the barrier properties of gliadin with low water vapor and oxygen permeability (López-de-Dicastillo, Gómez-Estaca, López-Carballo, Gavara, & Hernández-Muñoz, 2023). Moreover, GPhy and GSPE<sub>5%</sub> had less PV values than that of GL. However, among the loaded-fibers, GSPE<sub>5%</sub> was more effective against hydroperoxide molecules to suppress the formation of free radicals. Fig. 4b illustrates TBA test which had also the promising results similar to the PV measurement. According to the result of 15th week, GL ( $11.0\text{ meq/kg}$ ), GPhy ( $9.9\text{ meq/kg}$ ), and GSPE<sub>5%</sub> ( $9.8\text{ meq/kg}$ ) had better activities against oxidation than the control sample ( $13.3\text{ meq/kg}$ ). Despite the protective effect of GL, GPhy and GSPE<sub>5%</sub> also showed lower values in terms of antioxidative effects. Similar results were reported by Aydogdu, Sumnu, et al. (2019); Aydogdu, Yildiz, et al. (2019), showing that gallic acid-loaded hydroxypropyl methylcellulose- and lentil flour-based electrospun fibers were able to protect walnuts from oxidation in comparison with uncoated samples at  $40\text{ }^\circ\text{C}$  for 21 days.

## 4. Conclusion

The current research confirmed the capability of GPhy and GSPE<sub>5%</sub> to reduce lipid oxidation of walnut kernels. SEM revealed the tubular shape of optimum fibers which had  $\sim 90\%$  loading efficiencies. Gliadin denaturation by acetic acid was shown by simulation where instability, unfolding, and helix-to-coil transition were observed. Moreover, the chemical changes and enhanced thermostabilization of thermo-susceptible SPE after electrospinning were concluded. The fibers had bactericidal activities against *E. coli* and *S. aureus* bacteria as well as free radicals to provide their bactericidal and antioxidant capacities. Eventually, packaging application of the fibers during an accelerated storage test indicated that GPhy and GSPE<sub>5%</sub> effectively reduced lipid oxidation indices of the PV and TBA values during 15 weeks, proving their ability to overcome the lipid oxidation. Therefore, this study developed promising active food packaging materials by a one-step process and natural compounds, which were able to delay the lipid oxidation of walnut kernels.

### CRediT authorship contribution statement

Mohammad-Taghi Golmakani: Writing – review & editing,

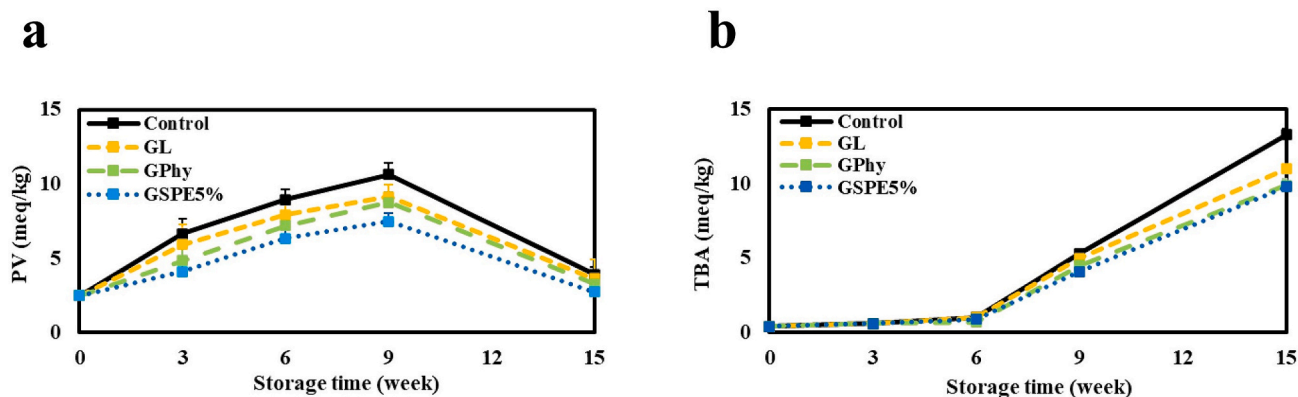


Fig. 4. (a) Peroxide value (PV) and (b) thiobarbituric acid (TBA) of coated and control walnut kernel samples during the accelerated storage period.

Validation, Supervision, Resources, Project administration, Funding acquisition, Conceptualization. **Mohammad Mahdi Hajjari:** Writing – original draft, Visualization, Validation, Software, Investigation, Data curation. **Farzaneh Kiani:** Writing – original draft, Software, Methodology, Investigation, Formal analysis, Data curation. **Niloufar Sharif:** Validation, Software, Methodology, Data curation, Conceptualization. **Seyed Mohammad Hashem Hosseini:** Validation, Supervision, Resources, Project administration, Methodology, Funding acquisition.

#### Declaration of competing interest

The authors declare that they have no known competing financial interests or personal relationships that could have appeared to influence the work reported in this paper.

#### Data availability

Data will be made available on request.

#### References

- Akman, P. K., Bozkurt, F., Balubaid, M., & Yilmaz, M. T. (2019). Fabrication of curcumin-loaded gliadin electrospun nanofibrous structures and bioactive properties. *Fibers and Polymers*, 20, 1187–1199.
- Alum, E. A., Urom, S., & Ben, C. M. A. (2016). Microbiological contamination of food: The mechanisms, impacts and prevention. *International Journal of Scientific & Technology Research*, 5(3), 65–78.
- Anandakrishnan, R., Aguilar, B., & Onufriev, A. V. (2012). H++ 3.0: Automating p K prediction and the preparation of biomolecular structures for atomistic molecular modeling and simulations. *Nucleic Acids Research*, 40(W1), W537–W541.
- Asghari, A., Fazilati, M., Latifi, A. M., Salavati, H., & Choopani, A. (2016). A review on antioxidant properties of Spirulina. *Journal Of Applied Biotechnology Reports*, 3(1), 345–351.
- Aydogdu, A., Sumnu, G., & Sahin, S. (2019). Fabrication of gallic acid loaded Hydroxypropyl methylcellulose nanofibers by electrospinning technique as active packaging material. *Carbohydrate Polymers*, 208, 241–250.
- Aydogdu, A., Yildiz, E., Aydogdu, Y., Sumnu, G., Sahin, S., & Ayhan, Z. (2019). Enhancing oxidative stability of walnuts by using gallic acid loaded lentil flour based electrospun nanofibers as active packaging material. *Food Hydrocolloids*, 95, 245–255.
- Benkert, P., Biasini, M., & Schwede, T. (2011). Toward the estimation of the absolute quality of individual protein structure models. *Bioinformatics*, 27(3), 343–350.
- Chen, T., Liu, H., Deng, C., Zhang, D., Li, H., Zhou, C., & Hong, P. (2023). Gelatin/wheat gliadin electrospun film containing Chlorogenic acid: Fabrication, characterization, and application in the preservation of grass carp (*Ctenopharyngodon idella*) filets. *Food Biophysics*, 1–16.
- Chentir, I., Hamdi, M., Li, S., Doumandji, A., Markou, G., & Nasri, M. (2018). Stability, bio-functionality and bio-activity of crude phycocyanin from a two-phase cultured Saharian *Arthrospira* sp. strain. *Algal Research*, 35, 395–406.
- Choudhary, S., Tanwer, B., Singh, T., & Vijayvergia, R. (2013). Total phenolic, total flavonoid content and the DPPH free radical scavenging activity of *Melothria maderaspatana* (Linn.) Cogn. *International Journal of Pharmacy and Pharmaceutical Sciences*, 5, 296–2986.
- Fernandes, R., Campos, J., Serra, M., Fidalgo, J., Almeida, H., Casas, A., ... Barros, A. I. (2023). Exploring the benefits of Phycocyanin: From Spirulina cultivation to its widespread applications. *Pharmaceuticals*, 16(4), 592.
- Ge, X., Huang, X., Zhou, L., & Wang, Y. (2022). Essential oil-loaded antimicrobial and antioxidant zein/poly (lactic acid) film as active food packaging. *Food Packaging and Shelf Life*, 34, Article 100977.
- Ghorani, B., & Tucker, N. (2015). Fundamentals of electrospinning as a novel delivery vehicle for bioactive compounds in food nanotechnology. *Food Hydrocolloids*, 51, 227–240.
- Hajimehdipoor, H., Shahrestani, R., & Shekarchi, M. (2014). Investigating the synergistic antioxidant effects of some flavonoid and phenolic compounds.
- Hajjari, M. M., Golmakani, M.-T., & Sharif, N. (2021). Fabrication and characterization of cuminaldehyde-loaded electrospun gliadin fiber mats. *LWT*, 145, Article 111373.
- Hajjari, M. M., Golmakani, M.-T., & Sharif, N. (2023). Electrospun zein/C-phycocyanin composite: Simulation, characterization and therapeutic application. *Food Hydrocolloids*, 140, Article 108638.
- Hajjari, M. M., Golmakani, M.-T., Sharif, N., & Niakousari, M. (2021). In-vitro and in-silico characterization of zein fiber incorporating cuminaldehyde. *Food and Bioproducts Processing*, 128, 166–176.
- Hajjari, M. M., & Sharif, N. (2021). In-silico behavior of dissolved prolamins under electric field effect applied by electrospinning process using molecular dynamics simulation. *Journal of Molecular Liquids*, 344, Article 117778.
- Hajjari, M. M., & Sharif, N. (2022). In-silico zein/tannic acid colloidal nanoparticles and their activity at oil and water interface of Pickering emulsion using molecular dynamics simulation. *Journal of Molecular Liquids*, 359, Article 119321.
- Kavitha, E., Stephen, L. D., Brishti, F. H., & Karthikeyan, S. (2021). Two-trace two-dimensional (2T2D) correlation infrared spectral analysis of *Spirulina platensis* and its commercial food products coupled with chemometric analysis. *Journal of Molecular Structure*, 1244, Article 130964.
- Kuai, L., Liu, F., Chiou, B.-S., Avena-Bustillos, R. J., McHugh, T. H., & Zhong, F. (2021). Controlled release of antioxidants from active food packaging: A review. *Food Hydrocolloids*, 120, Article 106992.
- Kumar, A., Ramamoorthy, D., Verma, D. K., Kumar, A., Kumar, N., Kanak, K. R., ... Mohan, K. (2022). Antioxidant and phytonutrient activities of *Spirulina platensis*. *Energy Nexus*, 6, Article 100070.
- Kumar, A., & Sinha-Ray, S. (2018). A review on biopolymer-based fibers via electrospinning and solution blowing and their applications. *Fibers*, 6(3), 45.
- Larrosa, A. P. Q., Camara, A. S., Pohndorf, R. S., da Rocha, S. F., Pinto, L. A., & d. A. (2018). Physicochemical, biochemical, and thermal properties of *Arthrospira* (*Spirulina*) biomass dried in spouted bed at different conditions. *Journal of Applied Phycology*, 30, 1019–1029.
- López-de-Dicastillo, C., Gómez-Estaca, J., López-Carballo, G., Gavara, R., & Hernández-Muñoz, P. (2023). Agro-industrial protein waste and co-products valorization for the development of bioplastics: Thermoprocessing and characterization of feather keratin/gliadin blends. *Molecules*, 28(21), 7350.
- Lu, X., Wang, J., Al-Qadiri, H. M., Ross, C. F., Powers, J. R., Tang, J., & Rasco, B. A. (2011). Determination of total phenolic content and antioxidant capacity of onion (*Allium cepa*) and shallot (*Allium oshananii*) using infrared spectroscopy. *Food Chemistry*, 129(2), 637–644.
- Mohamed, S. A., Osman, A., Abo Eita, A., & Sitohy, M. Z. (2018). Estimation of antibacterial and antioxidant activities of phycocyanin isolated from *Spirulina*. *Zagazig Journal of Agricultural Research*, 45(2), 657–666.
- Moreira, J. B., Lim, L.-T., da Rosa Zavareze, E., Dias, A. R. G., Costa, J. A. V., & de Moraes, M. G. (2019). Antioxidant ultrathin fibers developed with microalga compounds using a free surface electrospinning. *Food Hydrocolloids*, 93, 131–136.
- Moreno, M. A., Orqueda, M. E., Gómez-Mascaraque, L. G., Isla, M. I., & López-Rubio, A. (2019). Crosslinked electrospun zein-based food packaging coatings containing bioactive chilito fruit extracts. *Food Hydrocolloids*, 95, 496–505.
- Neo, Y. P., Swift, S., Ray, S., Gizdavic-Nikolaidis, M., Jin, J., & Perera, C. O. (2013). Evaluation of gallic acid loaded zein sub-micron electrospun fiber mats as novel active packaging materials. *Food Chemistry*, 141(3), 3192–3200.
- Onyeaka, H., Ghosh, S., Obileke, K., Miri, T., Odeyemi, O. A., Nwaiwu, O., & Tamasiga, P. (2024). Preventing chemical contaminants in food: Challenges and prospects for safe and sustainable food production. *Food Control*, 155, Article 110040.

- Park, E.-S., Moon, W.-S., Song, M.-J., Kim, M.-N., Chung, K.-H., & Yoon, J.-S. (2001). Antimicrobial activity of phenol and benzoic acid derivatives. *International Biodeterioration & Biodegradation*, 47(4), 209–214.
- Poggetti, L., Ferfuaia, C., Chiabà, C., Testolin, R., & Baldini, M. (2018). Kernel oil content and oil composition in walnut (*Juglans regia* L.) accessions from North-Eastern Italy. *Journal of the Science of Food and Agriculture*, 98(3), 955–962.
- Sabaghi, M., Maghsoudlou, Y., Khomeiri, M., & Ziaifar, A. M. (2015). Active edible coating from chitosan incorporating green tea extract as an antioxidant and antifungal on fresh walnut kernel. *Postharvest Biology and Technology*, 110, 224–228.
- Sabbaghi, S., & Mehravar, S. (2015). Effect of using nano encapsulated phase change material on thermal performance of micro heat sink. *International Journal of Nanoscience and Nanotechnology*, 11(1), 33–38.
- Sharif, N., Golmakani, M. T., & Hajjari, M. M. (2022). Integration of physicochemical, molecular dynamics, and in vitro evaluation of electrosprayed  $\gamma$ -oryzanol-loaded gliadin nanoparticles. *Food Chemistry*, 395, Article 133589.
- Sharif, N., Golmakani, M.-T., Hajjari, M. M., Aghaee, E., & Ghasemi, J. B. (2021). Antibacterial cuminaldehyde/hydroxypropyl- $\beta$ -cyclodextrin inclusion complex electrospun fibers mat: Fabrication and characterization. *Food Packaging and Shelf Life*, 29, Article 100738.
- Sharma, A., Noki, S., Zamisa, S. J., Hazzah, H. A., Almarhoon, Z. M., El-Faham, A., ... Albericio, F. (2018). Exploiting the thiobarbituric acid scaffold for antibacterial activity. *ChemMedChem*, 13(18), 1923–1930.
- Srinivas, G., Ochiye, H., & Mohan, R. (2014). Biomolecules in binary solvents: Computer simulation study of lysozyme protein in ethanol-water mixed solvent environment. *JSM Nanotechnol Nanomed*, 2(2), 10–29.
- Usharani, G., Srinivasan, G., Sivasakthi, S., & Saranraj, P. (2015). Antimicrobial activity of *Spirulina platensis* solvent extracts against pathogenic bacteria and fungi. *Advances in Biological Research*, 9(5), 292–298.
- Walker, S. S., & Black, T. A. (2021). Are outer-membrane targets the solution for MDR gram-negative bacteria? *Drug Discovery Today*, 26(9), 2152–2158.
- Xu, D., & Zhang, Y. (2012). Ab initio protein structure assembly using continuous structure fragments and optimized knowledge-based force field. *Proteins: Structure, Function, and Bioinformatics*, 80(7), 1715–1735.